# Observer-based robust integral of the sign of the error control of class I of underactuated mechanical systems: Theory and real-time experiments

Afef Hfaiedh, Ahmed Chemori, Afef Abdelkrim

Journal Title
XX(X):2–31

DOI: 10.1177/ToBeAssigned
www.sagepub.com/
SAGE

# Observer-Based RISE Control of Class I of Underactuated Mechanical Systems: Theory and Real-Time Experiments

**Afef Hfaiedh[1] and Ahmed Chemori[2] and Afef Abdelkrim[1]**

**Abstract**

In this paper, the control problem of a class I of underactuated mechanical systems is addressed. The considered class includes nonlinear underactuated mechanical systems with two degrees of freedom and one control input. Firstly, we propose the design of a Robust Integral of the Sign of the Error (RISE) control law, adequate for this special class. Based on a change of coordinates, the dynamics is transformed into a strict-feedback form. A Lyapunov-based technique is then employed to prove the asymptotic stability of the resulting closed-loop system. Numerical simulation results show the robustness and performance of the original RISE toward parametric uncertainties and disturbance rejection. A comparative study with a conventional sliding mode control reveals a significant robustness improvement with the proposed original RISE controller. However, in real-time experiments, the amplification of the measurement noise is a major problem. It has an impact on the behavior of the motor and reduces the performance of the system. To deal with this issue, we propose to estimate the velocity using the robust Levant differentiator instead of the numerical derivative. Real-time experiments were performed on the testbed of the inertia wheel inverted pendulum to demonstrate the relevance of the proposed observer-based RISE control scheme. The obtained real-time experimental results and the obtained evaluation indices show clearly a better performance of the proposed observer-based RISE approach compared to the sliding mode and the original RISE controllers.

**Keywords**

Underactuated mechanical systems, RISE feedback control, strict-feedback form, Levant differentiator, Inertia Wheel Inverted Pendulum.

*Prepared using* **sagej.cls** *[Version: 2017/01/17 v1.20]*

## Introduction

Control of Underactuated Mechanical Systems (UMSs) has got over the years a growing attention within the automatic control community (Fantoni and Lozano (2002)). The presence of underactuation in mechanical systems can be due to various reasons (Choukchou-Braham et al. (2014)). It may be intentionally specified during the design stage to minimize the weight of the system. Otherwise, it may be unintentional, as a result of the damage of one actuator or more of the system. The underactuation in mechanical systems gives rise to various challenging control issues, (Krafes et al. (2018)), including:

- Many difficulties are often exhibited by such systems, such as their complex dynamics and their nonlinear coupling between actuated and non-actuated coordinates.
- Non-integrable and second-order non-holonomic constraints that may exist in the dynamics of UMSs. For instance, the dynamic model of the pendubot is subject to second-order non-integrable differential constraints.
- UMSs are often considered as a non-minimum phase, as the internal dynamics of such systems is often unstable. Hence, the application of I/O feedback linearization is not efficient to control such systems (Guemghar (2005)).
- One of the control challenges is the lack of feedback linearizability. For instance, the dynamic model of the acrobot (Spong (1995)) and the pendubot (Zhang and Tarn (2001)) systems are not feedback linearizable with a static state feedback. However, only a partial feedback linearization is possible in such cases.

Due to their different structural properties, UMSs are studied in a separate way and there is no general approach to control all variants of them. Some classifications of these systems have been reported in the literature. For instance, in (Seto and Baillieul (1994)) the authors proposed three representations called tree, isolated vertex and chain, classified using the method of the control flow diagram. It is a graphical representation of the dynamics which represents the interaction forces through the degrees of freedom. Another classification was proposed in (Olfati-Saber (2001)), using some structural properties of the

[1]University of Carthage, National Engineering School of Carthage (ENICarthage), LR18ES44 Research Laboratory Smart Electricity & ICT, SE&ICT Lab, Tunis, Tunisia
[2]LIRMM, University of Montpellier, CNRS, Montpellier, France

**Corresponding author:**
Afef Hfaiedh University of Carthage, National Engineering School of Carthage (ENICarthage), LR18ES44 Research Laboratory Smart Electricity & ICT, SE&ICT Lab, Tunis, Tunisia
Email: afef.hfaiedh@enicar.u-carthage.tn

*Prepared using* sagej.cls

system like kinetic symmetry, interacting inputs, etc. The author proposed three normal representations for 2-DOF systems where a backstepping procedure and a forwarding scheme were developed for the feedback form and the feed-forward form respectively. Besides, a wide range of control techniques have been proposed in the literature, such as partial feedback linearization (Spong and Praly (1997)), passivity-based-control (Ortega et al. (2002) and Donaire et al. (2017)), adaptive neural network-based control (Moreno-Valenzuela et al. (2017) and Ghommam and Chemori (2017)), optimization-based-control (Andary et al. (2009)), observer-based super-twisting control (Hfaiedh et al. (2020a)), to name a few.

One particular control approach, mostly used to address the control issue of perturbed UMSs, is the sliding mode control (SMC). It is a robust control strategy characterized by its invariance toward some model uncertainties and external disturbances (Utkin (2008)). Various SMC approaches were proposed in the literature for UMSs. After representation of the system model into a quasi-chained form, a nonlinear robust SMC controller was proposed in (Lu et al. (2016) and Sun et al. (2015)) to make the system states driven to reach the sliding manifold, and guarantee their convergence to the equilibrium point. In (Khalid and Memon (2016)), a first-order SMC with a high-gain observe has been proposed for the stabilization of the inertia wheel inverted pendulum (IWIP). In (Cheng and Ho (2017)) an adaptive sliding mode controller was designed for a class of nonlinear UMSs with matched and mismatched disturbances. Another SMC scheme based on an extended disturbance observer was proposed in (Ding et al. (2017)) to control a second-order UMS. Thakar et al. (2013) propose a sliding mode approach to control an underactuated system based on the nonlinear model of lateral slosh-container. The main drawback of the first order (SMC) control is the so-called chattering phenomenon. From a practical point of view, this effect is undesirable, since it involves a high control activity generated by the high-frequency of unmodeled dynamics (Slotine and Li (1991)).

To overcome this problem, we are interested in this paper, to redesign another nonlinear robust controller, namely the Robust Integral of the Sign of the Error (RISE) controller (Xian et al. (2004)). Compared to the SMC, RISE feedback control generates a continuous control law and prevents the chattering phenomenon due to the integral of the discontinuous term in the expression of the control law (Fischer et al. (2014)). It has also the advantage to compensate sufficiently smooth nonlinear disturbances and system uncertainties. Various theoretical extensions of this control scheme have been proposed in the literature, and were applied to a wide range of systems, including autonomous underwater vehicles (Fischer et al. (2014)), multi-link flexible manipulators (Jian et al. (2014)), parallel robots (Bennehar et al. (2018)), Hard Disc Drives (Taktak-Meziou et al. (2014)), underactuated mechanical systems (Hfaiedh et al. (2018)), exoskeletons (Sherwani et al. (2020)).

The main contributions of the present paper can be summarized as follows:

1. This work is an extension of the conference paper of (Hfaiedh et al. (2018)), where a RISE controller was applied to a 2-DOF underactuated inertia wheel inverted pendulum. The new findings of this paper include (i) the proof of the stability analysis of the resulting closed-loop system, (ii) new simulations and real-time experimental results and (iii) quantification of the performance through various performance evaluation indices.
2. The first contribution lies in the redesign of the RISE controller for underactuated mechanical systems. To the best of the authors' knowledge, no previous work in the literature has been dealt with RISE control to stabilize UMSs whose control design is more difficult than fully-actuated systems. The choice of designing RISE controller is motivated by the advantage of generating a continuous control law with a guaranteed closed-loop stability based on some trivial properties of the system dynamics. Compared to fully actuated systems, the proposed RISE control could not be straightforwardly applied to UMSs. Referring to the classification of (Olfati-Saber (2001)), we transform the system into a strict-feedback form, which decouples the original system into two cascaded nonlinear and linear subsystems. The new control input is included in the actuated subsystem, which is not the case for the unactuated subsystem. Then, new desired trajectories and tracking errors are defined according to the Lyapunov concept of the nonlinear subsystem.
3. Numerical simulations were conducted to demonstrate the robustness of the proposed RISE controller on the inertia wheel inverted pendulum (IWIP). Two scenarios have been performed in simulation test, the first one deals with robustness towards parametric uncertainties and the second one concerns external disturbance rejection. A comparative analysis between the first order sliding mode controller and the proposed original RISE controller is presented and discussed. Moreover, robustness evaluation indices are used to evaluate and compare each controller. This proposed extended version includes a confirmed simulation with a rigorous stability analysis of the resulting closed-loop system.
4. The second contribution focuses on improving the experimental results of the original RISE controller with a differentiator. It is worth noting that, the RISE controller can compensate for uncertainties. This is of a considerable importance for underactuated mechanical system, since uncertainties are extremely abundant in their dynamics. However, by computing the velocity signal using the numerical derivative of the measured position, an amplification of the measurement noise has been noticed. This noise effect has an impact on the behavior of the motor, so that it may reduce the system performance. Accordingly, we propose to estimate the angular velocity of the pendulum using a Levant differentiator, to reduce the effect of the measurement noise.
5. A comparative study between a first-order sliding mode controller, the original RISE controller and the observer-based RISE controller is validated experimentally on the benchmark of the inertia wheel inverted pendulum. Two different scenarios are conducted: in the first one, no additional

mass is added to the pendulum body. In the second, the system is exposed to more challenging external disturbances, compared to the previous work (Hfaiedh et al. (2018)), where only punctual disturbances were considered. The disturbances, in the second scenario, consist of an additional mass added to the pendulum body in two successive and close periods. It is an important scenario, as we can evaluate the performance of both the original RISE control and the proposed observer-based RISE control. A comparative analysis is also presented based on various evaluation indices to quantify the performance of the SMC and the original RISE controller with respect to the proposed approach in terms of convergence and energy consumption.

This paper is organized as follows: in the second section, we present a general background on Class I of nonlinear UMSs, represented in strict-feedback form, and give more details about the application of RISE feedback control. Section 3 is devoted to an example of application, provided to stabilize a second-order UMS with analytical proof of Lyapunov stability of the resulting closed-loop system. Numerical simulation results with different scenarios are presented and discussed in the forth section. In section 5, we present real-time experimental results to show the effectiveness of the proposed control approach combined with the Levant differentiator. Conclusion and future work are provided in section 6.

## Proposed control solution

### *Class I of underactuated mechanical systems*

Consider an underactuated mechanical system described by

$$D(q)\ddot{q}+C(q,\dot{q})\dot{q}+G(q)=F_e(q)\tau \tag{1}$$

where $\tau=[\tau_1,\tau_2]^T\in\mathbb{R}^m$ is the control input, $D(q)\in\mathbb{R}^{n\times n}$ is the inertia matrix, $C(q)\in\mathbb{R}^{n\times n}$ is the Coriolis and Centrifugal matrix, $G(q)\in\mathbb{R}^{n\times 1}$ is the gravity vector and $F_e(q)=[0,I_m]^T\in\mathbb{R}^{n\times m}$ ) denotes a non-square matrix of external forces with $m<n$. Assume that the configuration is partitioned into $q=(q_1,q_2)$ where $q_1\in\mathbb{R}^{n-m\times 1}$ is the non-actuated coordinates and $q_2\in\mathbb{R}^{m\times 1}$ is the actuated coordinates. UMSs with two degrees of freedom can be described as follows:

$$\begin{bmatrix} m_{11}(q) & m_{12}(q) \\ m_{21}(q) & m_{22}(q) \end{bmatrix}\begin{bmatrix} \ddot{q}_1 \\ \ddot{q}_2 \end{bmatrix}+\begin{bmatrix} h_1(q,\dot{q}) \\ h_2(q,\dot{q}) \end{bmatrix}=\begin{bmatrix} 0 \\ \tau \end{bmatrix} \tag{2}$$

where $m_{11}(q),m_{12}(q),m_{21}(q),m_{22}(q)$ represent the components of the inertia matrix and $h_1(q,\dot{q}),h_2(q,\dot{q})$ contain the Coriolis, Centrifugal and gravity terms. Generally, underactuated mechanical systems in the form (2) are not fully feedback linearizable and conventional control approaches could not be

straightforwardly applied to such systems. Based on a global change of coordinates, the system (2) can be transormed into a cascade form. With this transformation, the control input can act on both actuated and non-actuated coordinates.

Due to the lack of actuation in the first equation of (2), the system belongs to the class I, otherwise, it belongs to the class II according to the classification of (Olfati-Saber (2001)). For instance, the TORA (Translational Oscillator Rotational Actuator) system, the acrobot (Zhao and Yi (2006)) and the IWIP belong to the class I, whereas the cart pole inverted pendulum and the pendubot belong to the class II. The main motivation of this classification is to obtain a general transformation of the system model into other simplified representation which makes the control problem more simplified. For instance, the class I can be partially linearized and then transformed into a strict-feedback form, leading to a double integrator thanks to the lack of control input in the first equation of (2). This linearization method is known as collocated partial feedback linearization (Spong (1994)). In next section, we present a brief background on the transformation of class I of UMSs into a strict-feedback form.

Definition 1: A nonlinear system presented into a strict-feedback form (Krstic et al. (1995)) can be described by the following triangular structure.

$$\dot{z} = f(z, \xi_1) \tag{3}$$

$$\dot{\xi}_1 = \xi_2 \tag{4}$$

$$\dot{\xi}_{n-1} = \xi_n \tag{5}$$

$$\dot{\xi}_n = u \tag{6}$$

where $(z, \xi_1, \xi_2, ..., \xi_n)$ is the composite state, $f$ is a nonlinear function and $u$ is the control input. $\dot{z}, \dot{\xi}_1, ..., \dot{\xi}_{n-1}$ equations only depend on states $z, \xi_1, ..., \xi_i$ that are fed back to that subsystem.

## *Background on RISE controller for class I of underactuated mechanical systems*

The main motivation behind this section is to give a background about the design of the RISE controller using the global change of coordinates which simplifies the control problem by transforming the system into a strict-feedback form.

*Strict feedback linearization:* Underactuated mechanical systems of class I with two degrees of freedom and only one control input can be represented into a cascaded nonlinear system in the strict-feedback representation if the following assumption is satisfied.

**Assumption 1**: Using the Lagrangian of the system, its configuration is partitioned into $q = (q_1, q_2)$ and if the quantity $m_{11}^{-1}(q_2)m_{12}(q_2)$ is integrable, a global change of coordinates can be obtained as

follows:

$$\begin{aligned} z_1 &= q_1 + \gamma(q_2) \\ z_2 &= m_{11}(q_2)p_1 + m_{12}(q_2)p_2 \\ \xi_1 &= q_2 \\ \xi_2 &= p_2 \end{aligned} \tag{7}$$

where $p_1 = \dot{q}_1$, $p_2 = \dot{q}_2$, $\gamma(q_2) = \int_0^{q_2} m_{11}^{(-1)}(\theta)m_{12}(\theta)\partial\theta$ and $[z_1, z_2, \xi_1, \xi_2]^T$ is the novel state vector. Using the new states, we obtain a new representation of the system composed of a linear (double integrator) subsystem and a nonlinear core subsystem (Olfati-Saber (2001)). The new system representation is then described as follows:

$$\dot{z}_1 = m_{11}^{-1}(\xi_1)z_2 \tag{8}$$

$$\dot{z}_2 = g_1(z_1 - \gamma(\xi_1), \xi_1) \tag{9}$$

$$\dot{\xi}_1 = \xi_2 \tag{10}$$

$$\dot{\xi}_2 = u \tag{11}$$

where $g_1(q_1, q_2) = -\frac{\partial V(q)}{\partial q_1}$ , $V(q)$ denotes the potential energy of the system and $u$ is the new control input from collocated partial feedback linearization. The relation between the torque and the new control term is described through the following expressions:

$$\tau = \Theta(q)u + \Upsilon(q, \dot{q}) \tag{12}$$

$$\Theta(q) = m_{22}(q) - m_{21}(q)m_{11}^{-1}(q)m_{12}(q) \tag{13}$$

$$\Upsilon(q, \dot{q}) = h_2(q, \dot{q}) - m_{21}m_{11}^{-1}(q)h_1(q, \dot{q}) \tag{14}$$

*Proposed RISE control design approach for class I of underactuated mechanical systems:* RISE feedback control was successfully applied to fully actuated systems, and was validated as a promising control technique. The main motivation of this paper is to propose a new redesign of the RISE feedback control for a more complex and challenging systems like the class I of UMSs. The following hypotheses are essential to ensure the design of the proposed nonlinear RISE controller. Consider the dynamics of a nonlinear system described by the following form:

$$M(x, \dot{x}, ..., x^{n-1})x^n + F(x, \dot{x}, ..., x^{n-1}) = U(t) \tag{15}$$

where $(.)^{(i)}(t)$ denotes the $i^{th}$ time derivative of $(.)$, $U$ represents the control input vector, $X = [x, \dot{x}, ..., x^{n-1}, x^n] \in \mathbb{R}^n$ is the state vector, $M$ and $F \in \mathbb{R}^n$ are uncertain nonlinear functions.

**Property 1**: The uncertain nonlinear function matrix $M$ satisfies the following inequality.

$$\underline{m}\|\xi\|^2 \leq \xi^T M(.)\xi \leq \overline{m}(q)\|\xi\|^2 \tag{16}$$

$M(.)$ is bounded from below by a positive constant $\underline{m}$ and from above by a non-decreasing positive function $\overline{m}(q)$.

**Property 2**: The two functions $M(.)$ and $F(.)$ of the nonlinear system (15) are second-order differentiable.

**Property 3**: The desired reference trajectory is continuously differentiable with respect to time, up to the $(n+2)^{th}$ derivative.

The expression of RISE control law requires some auxiliary error signals, denoted by $e_i(t), i = 1, 2$ and defined in the following manner:

$$e_1 \triangleq q_d - q \tag{17}$$

$$\dot{e}_1 \triangleq \dot{q}_d - \dot{q} \tag{18}$$

$$e_2 \triangleq \dot{e}_1 + \alpha_1 e_1 \tag{19}$$

$$r \triangleq \dot{e}_2 + \alpha_2 e_2 \tag{20}$$

where the two constant gains $\alpha_1$ and $\alpha_2$ are positive. $q_d$ and $\dot{q}_d$ are the desired trajectory and its first time derivative respectively. Some systems are not equipped with sensors required to measure acceleration forces due to their very high cost. So this quantity can be derived by differentiating the velocity signal. However, the limitation of this method is its high sensitivity to noise, as a low level of noise in the velocity signal can lead to an amplified noise in the estimated acceleration signal. For this reason, in this case, the auxiliary error signal $r(t)$ is not used in the control design since it requires a numerical differentiation through the computational algorithm to obtain the second derivative of the position signal which is foremost a noisy signal. One practical solution to attenuate the noise level in the velocity estimation is proposed in the forthcoming section. The expression of the RISE control law is expressed as follows (Xian et al. (2004) and Fischer et al. (2014)):

$$\begin{aligned} u &= (k_s + 1)e_2 - (k_s + 1)e_2(0) + \nu_f \\ \dot{\nu}_f &= (k_s + 1)\alpha_2 e_2 + \beta sign(e_2) \\ \nu_f(0) &= 0 \end{aligned} \tag{21}$$

where the two constant gains $k_s$ and $\beta$ are positive and *sign* function denotes the mathematical Signum function described as

$$sign(x) = \begin{cases} 0 & \text{if } x = 0 \\ \frac{x}{|x|} & \text{if } x \neq 0 \end{cases}$$

### *State estimation with robust Levant differentiator*

The presence of noise in measured signals is inevitable in any real-time experimental application. It certainly affects the performance of the system, especially when computing the first and second time derivatives of those noisy measured signals. To overcome this problem, we propose to use the differentiator of (Levant (2003)) to provide the derivatives required to implement the RISE controller. The choice of the differentiator is motivated by its high precision and robustness in the presence of noise and parametric uncertainties (Imine et al. (2011)). The differentiator of (Levant (2003)) is described as follows:

$$\dot{w}_0 = v_0 \tag{22}$$

$$v_0 = w_0 - \lambda_2 L^{\frac{1}{3}} |w_0 - y|^{\frac{2}{3}} sign(w_0 - y) \tag{23}$$

$$\dot{w}_1 = v_1 \tag{24}$$

$$v_1 = w_1 - \lambda_1 L^{\frac{1}{2}} |w_1 - v_0|^{\frac{1}{2}} sign(w_1 - v_0) \tag{25}$$

$$\dot{w}_2 = -\lambda_0 L sign(w_2 - v_1) \tag{26}$$

If $t = 0$, $w_0 = y$ and $w_1(0) = w_2(0) = 0$. $y$ is the output of the system, $w_0$ is the estimated output. $w_1$ is its first time derivative and $w_2$ is its second time derivative. The gains $L$, $\lambda_0$, $\lambda_1$ and $\lambda_2$ are positive. In next section, we propose to design the RISE controller using a global change of coordinates for the Inertia Wheel Inverted Pendulum (IWIP) and present the Lyapunov stability analysis of the closed-loop system. We also demonstrate the use of the resulting Levant differentiator in real-time experiments.

## Application example : IWIP

The design of the proposed RISE controller using a global change of coordinates combined with the Levant differentiator is presented in this section. An application example of this control approach is illustrated on a second-order underactuated mechanical system. A brief description of the system, the control design and the stability analysis are introduced in this section.

## Description of the inertia wheel inverted pendulum

The inertia wheel inverted pendulum (see **Figure** 1) has attracted the attention of many researchers within the control community (Freidovich et al. (2009) and Zhang et al. (2016)). It was considered a lot as a benchmark to study new nonlinear approaches (Moreno-Valenzuela et al. (2017) ;Estrada et al. (2012); Andary et al. (2012); Haddad et al. (2018); Gritli et al. (2017); Aguilar-Avelar et al. (2017)). It has the flatness property with kinetic symmetry (Olfati-Saber (2001)). The pendulum angle $\theta_1$ with respect to vertical axis is unactuated and the angle between the body and the inertia wheel $\theta_2$ is actuated. The configuration in which the pendulum is pointed upwards corresponds to the unstable equilibrium point. Suppose that the torque $\tau_a$ is the sum of the torque acting at $O$ and generated by the force $F^+$ and $\tau_b$ is the sum of the torques generated by both the gravity $P$ and $F^-$ forces.

To straighten up the pendulum, the torque $\tau_a$ must be greater than $\tau_b$. An angular acceleration is produced by the motor torque acting on the rotating wheel, consequently, due to the dynamic coupling, a torque acting on the passive joint is generated. Therefore, the objective is to design a control acting on the inertia wheel to steer and maintain the pendulum in its unstable equilibrium point. The equation of

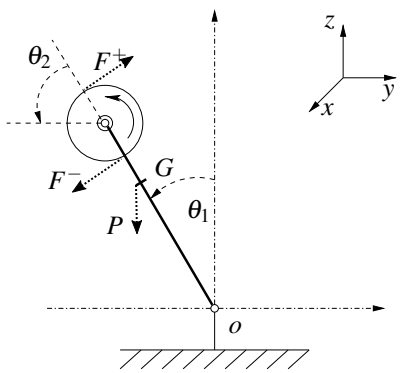


**Figure 1.** Schematic view of the system: the first joint $\theta_1$ is unactuated, while the second one $\theta_2$ is actuated.

motion of the system is obtained using the Euler–Lagrange method. The Lagrangian expression of this system is given by:

$$L = \frac{1}{2}(I_0\dot{\theta}_1^2 + i_2(\dot{\theta}_1 + \dot{\theta}_2)^2) - m_0 g\cos(\theta_1) \tag{27}$$

where $\theta_1$ and $\theta_2$ denote,respectively, the angular position of the pendulum and the angular position of the inertia wheel, $\dot{\theta}_1$ and $\dot{\theta}_2$ represent their corresponding velocities. The application of the Lagrange method

leads to the following dynamic model of the IWIP (Fantoni and Lozano (2002)):

$$\begin{bmatrix} I_0+i_2 & i_2 \\ i_2 & i_2 \end{bmatrix} \begin{bmatrix} \ddot{\theta}_1 \\ \ddot{\theta}_2 \end{bmatrix} - \begin{bmatrix} m_0 g \sin(\theta_1) \\ 0 \end{bmatrix} = \begin{bmatrix} 0 \\ \tau \end{bmatrix} \tag{28}$$

where $\tau$ is the torque applied on the active joint of the system. The parameters of this second-order underactuated mechanical system are summarized in **Table** 1. The expressions of the two constants $I_0$ and $m_0$ are given by:

$$I_0 = ml^2 + ML^2 + i_1 \tag{29}$$

$$m_0 = ml + ML \tag{30}$$

**Table 1.** Summary of the dynamic parameters of the IWIP

| Parameter | Description | Value |
|---|---|---|
| $i_1$ | Body inertia | $0.031468[kg.m^2]$ |
| $i_2$ | Wheel inertia | $4.17610^{-4}[kg.m^2]$ |
| $l$ | Body center of mass position | $0.06[m]$ |
| $L$ | Wheel center of mass position | $0.044[m]$ |
| $m$ | Body mass | $3.228[kg]$ |
| $M$ | Wheel mass | $0.86422[kg]$ |
| $g$ | Constant of gravitational acceleration | $9.8[m.s^{-2}]$ |

## *The control design*

The dynamic model (28) satisfies **Assumption 1**, since the inertia matrix is constant. Therefore, the global change of coordinates can be defined as follows:

$$z_1 = \frac{\partial L}{\partial \dot{\theta}_1} = (I_0+i_2)\hat{\dot{\theta}}_1 + i_2\dot{\theta}_2 \tag{31}$$

$$z_2 = \hat{\theta}_1 \tag{32}$$

$$z_3 = \dot{\theta}_2 \tag{33}$$

where $Z = [z_1, z_2, z_3]$ is the novel state vector, $\hat{\theta}_1, \hat{\dot{\theta}}_1$ are respectively the estimated angular position and velocity of the pendulum through the proposed Levant differentiator.

**Remark 1**: The observer is used to estimate the angular velocity of the pendulum. In fact, by computing

the velocity signal using the numerical derivative of the measured position of the pendulum, an amplification of the measurement noise has been noticed. This noise effect has an impact on the behavior of the actuator, so that it may reduce the performance of the closed-loop system. Accordingly, we propose to estimate both the angular position and the velocity of the pendulum using a differentiator, to obtain a more smooth velocity and control input signals.

Using the change of coordinates, the system is transformed into a strict-feedback form as follows:

$$\dot{z}_1 = \frac{\partial L}{\partial \theta_1} = m_0 g \sin(z_2) \tag{34}$$

$$\dot{z}_2 = \frac{z_1}{I_0 + i_2} - \frac{i_2 z_3}{I_0 + i_2} \tag{35}$$

$$\dot{z}_3 = u \tag{36}$$

With this new strict-feedback representation, the control input can act on both actuated and unactuated coordinates. The resulting system is presented as a cascade connection between a linear and a nonlinear subsystem where $z_2$ is considered as a virtual control input of the nonlinear $z_1$-subsystem. Lyapunov analysis is adopted to make the nonlinear-subsystem represented by (34) globally asymptotically stable. Assume that the desired trajectory for the $z_1$-subsystem described as a sigmoidal function and its first derivative are expressed as follows:

$$\theta_{1d} = z_{2d} = -\arctan(z_1) \tag{37}$$

$$\dot{\theta}_{1d} = \frac{m_0 g \sin(z_2)}{(1 + (z_1^2))} \tag{38}$$

Taking the time derivative of the Lyapunov candidate (40), we obtain

$$\dot{V}(z_1) = z_1 \dot{z_1} \tag{39}$$

Let a valid Lyapunov function expressed as follows.

$$V(z_1) = \frac{z_1^2}{2} \tag{40}$$

we substitute $\dot{z}_1$ by its expression (34) into (39), then we add the expression of (37). After some trigonometric simplifications, we obtain:

$$\dot{V}(z_1) = z_1 m_0 g \sin(z_2) \tag{41}$$

$$\dot{V}(z_1) = z_1 m_0 g \sin(-\arctan(z_1)) \tag{42}$$

$$\dot{V}(z_1) = -z_1 m_0 g \frac{z_1}{\sqrt{1+z_1^2}} \tag{43}$$

Based on Lyapunov function (40), we can conclude that the choice of the desired sigmoid function (37) can globally stabilize the nonlinear subsystem (34).

if $z_1 > 0$, then, $\dot{V}(z_1) < 0$

if $z_1 = 0$, then, $\dot{V}(z_1) = 0$

if $z_1 < 0$, then, $\dot{V}(z_1) < 0$

The proposed desired trajectories can now be used for the design of the RISE controller. The control law expressed in (21) depends on the auxiliary errors $\hat{e}_1$ and $\hat{e}_2$. Replacing (37) and (38) in (17) and substituting $\theta$ and $\dot{\theta}$ by their estimates $\hat{\theta}$ and $\hat{\dot{\theta}}$, gives:

$$\hat{e}_1 = \hat{\theta}_1 - \theta_{1d} \tag{44}$$

$$\hat{\dot{e}}_1 = \hat{\dot{\theta}}_1 - \dot{\theta}_{1d} \tag{45}$$

$$\hat{e}_2 = \hat{\dot{e}}_1 - \alpha_1 \hat{e}_1 \tag{46}$$

where $\theta_{1d}$ denotes the desired trajectory and its first derivative is $\dot{\theta}_{1d}$. $\hat{\theta}$ and $\hat{\dot{\theta}}$ are respectively the estimated pendulum position and velocity generated by the proposed Levant differentiator.

Using the equations (44) and (21), the control input designed, based on the estimated states, can be expressed by:

$$u = (k_s+1)\hat{e}_2 - (k_s+1)\hat{e}_2(0) + \nu_f \tag{47}$$

$$\dot{\nu}_f = (k_s+1)\alpha_2 \hat{e}_2 + \beta sign(\hat{e}_2) \tag{48}$$

**Figure** 2 illustrates the block diagram of the proposed control approach based on Levant differentiator.

## *Closed-loop stability analysis*

By replacing the expression $\ddot{\theta}_2$ in the first part of the equation (28), we obtain the same form as in (15) $m(q)\ddot{\theta}_1 + f(\theta_1) = u$, where $m(q) = I_0 + i_2$ and $f(\theta_1) = -m_0 g sin(\theta_1)$. Using properties 1-3 and following

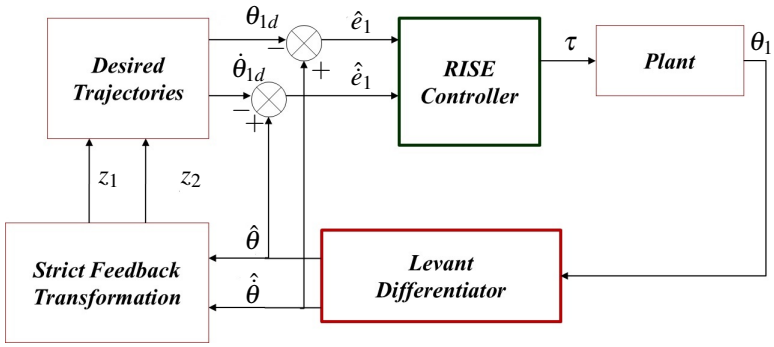


**Figure 2.** View of the block diagram of the proposed control approach.

the same reasoning in (Xian et al. (2004)), the stability of the RISE controller is demonstrated. We consider that the desired joint positions, velocities and accelerations are denoted respectively by $q_d(t)$, $\dot{q}_d(t)$ and $\ddot{q}_d(t)$. Taking the expressions of the tracking errors in (17), the filtered tracking error $r(t)$ is expressed by

$$r = \dot{e}_2 + \alpha_2 e_2 \tag{49}$$

where $\alpha_2 > 0$ is a positive design constant parameter. Multiplying the first derivative of (49) by $M(q)$, we obtain the open-loop error system.

$$m(q)\dot{r} = -\frac{1}{2}\dot{m}(q)r - e_2 - \dot{u} + N \tag{50}$$

In our case, the inertia matrix is constant, then $\dot{m}(q) = 0$, the expression (50) becomes:

$$m(q)\dot{r} = -e_2 - \dot{u} + N \tag{51}$$

where $N(.)$ denotes a nonlinear immeasurable auxiliary function expressed by

$$N(.) = m(q)\left(q_d^{(3)} + \alpha_2 \dot{e}_2\right) + e_2 + \dot{f}(q) \tag{52}$$

After taking the time derivative of the control input, we obtain:

$$\dot{u} = (k_s + 1)r + \beta sign(e_2) \tag{53}$$

By substituting (53) into (51), we obtain the following closed-loop system

$$m(q)\dot{r} = -e_2 - (k_s + 1)r - \beta sign(e_2) + N \tag{54}$$

Let us now consider an auxiliary function $N_d(.)$ expressed by:

$$N_d(.) = m(q)q_d^{(3)} + \dot{f}(q_d) \tag{55}$$

after we add and subtract the function $N_d(t)$ (55) to the right-hand side of the closed-loop error system (54), the following expression is obtained:

$$m(q)\dot{r} = -e_2 - (k_s + 1)r - \beta sign(e_2) + \tilde{N} + N_d \tag{56}$$

where $\tilde{N}$ is defined by:

$$\tilde{N} := N - N_d \tag{57}$$

with the function $N$ defined in (52) continuously differentiable and the function (57) can be upper bounded as follows:

$$\|\tilde{N}\| < \rho(\|z_\rho\|)\|z_\rho\| \tag{58}$$

where $\|z_\rho\|$ represents the Euclidean norm and $z_\rho(t)$ is defined as

$$z_\rho := [e_1, e_2, r]^T \tag{59}$$

where $\rho : \mathbb{R}_{\geq 0} \to \mathbb{R}_{\geq 0}$ is some non-decreasing and globally invertible function.

**Lemma 1**: Consider the expression of the auxiliary function $L(t) \in \mathbb{R}$ defined as :

$$L = r(N_d - \beta sign(e_2)) \tag{60}$$

If the control gain $\beta$ is chosen according to the following sufficient inequality expressed by:

$$\beta > \|N_d(t)\|_{L_\infty} + \frac{1}{\alpha_2}\|\dot{N}_d(t)\|_{L_\infty} \tag{61}$$

then

$$\int_0^t L(\tau)d\tau \leq \zeta_b \tag{62}$$

where $\|\|_{L_\infty}$ is the $L_\infty$ norm and $\zeta_b$ is a positive constant defined as

$$\zeta_b = \beta|e_2(0)| - e_2(0)N_d(0) \tag{63}$$

**Theorem 1:** The control law ensures that all system signals are bounded under closed-loop operation and

$$\|e(t)\| \quad \to 0 \quad as \quad t \to \infty, \tag{64}$$

provided that the control gain $\beta$ is selected according to (61), $\alpha_2 > \frac{1}{2}$ and the control gain $k_s$ is chosen sufficiently large relative to the system initial conditions.

**Proof**: Let us consider the auxiliary function $P(t) \in \mathbb{R}$ expressed as follows:

$$P(t) = \zeta_b - \int_0^t L(\tau)d\tau \tag{65}$$

where $\zeta_b$ and $L$ are defined in (63) and (60) respectively. We define now the Lyapunov candidate $V : \mathbb{R}^{n+1} \times \mathbb{R}_{\geq 0} \longrightarrow \mathbb{R}_{\geq 0}$ as follows

$$V(y,t) = \frac{1}{2}\sum_{j=1}^{n=2} e_j^2 + \frac{1}{2}mr^2 + P \tag{66}$$

where $y$ is defined as

$$y := [z_\rho^T \sqrt{P}]^T \tag{67}$$

and $z_\rho(t)$ is defined in (59). Since $m(q) > 0$ we deduce that

$$\underline{m} \leq m(q) \leq (\overline{m}(\|y\|)) \tag{68}$$

where $\underline{m}$ is a positive constant and $\overline{m}(q) : \quad \mathbb{R}_{\geq 0} \longrightarrow \mathbb{R}_{\geq 0}$ is some nondecreasing function (see **Property 1**). Therefore, we can bound (66) as follows

$$\lambda_1\|y\| \leq V \leq \lambda_2(\|y\|)\|y\|^2 \tag{69}$$

where $\lambda_1 = (1/2)min\{1, \underline{m}\}$ and $\lambda_2(\|y\|) := max\{(1/2)\overline{m}(\|y\|), 1\}$.

After taking the time derivative of (66), we obtain:

$$\dot{V} = -\alpha_2 e_2^2 + e_1 e_2 - r^2 + r\tilde{N} - K_s r^2 + [r(N_d - Bsign(e_2) - L] \tag{70}$$

where $\dot{P} = r(N_d - Bsign(e_2))$. By using the fact that $e_1 e_2 \geq (1/2)(e_1^2 + e_2^2)$ and (58) we can obtain an upper bound of (70) as follows:

$$\begin{aligned} \dot{V} &\leq -\lambda_3 \|z_\rho\|^2 + |r|\rho(\|z_\rho\|)\|z_\rho\| - k_s r^2 \\ \dot{V} &\leq -\left(\lambda_3 - \frac{\rho^2(\|z_\rho\|)}{4k_s}\right)\|z_\rho\|^2 \end{aligned} \tag{71}$$

where $\alpha_2 > 1/2$ and $\lambda_3 = min\{(1/2), \alpha_2 - (1/2)\}$

We can conclude from (71) that

$$\dot{V} \leq -\gamma \|z_\rho\|^2 \tag{72}$$

with $k_s > \frac{1}{4\lambda_3}\rho^2(\|z_\rho\|)$ and $\gamma$ some positive constant. Based on the lemma 2 of (Xian et al. (2004)), it can be verified that the closed-loop system states asymptotically converge to zero, thereby, $e_1 \to 0$, $e_2 \to 0, r \to 0$ as $t \to \infty$.

## Numerical Simulation results

In this section, we present simulation-based results applied to the IWIP to analyse the performance of the proposed control method without using the Levant differentiator. Two different simulation scenarios are proposed. In the first one, parametric uncertainties are introduced in some physical parameters of the system, whereas in the second one, a sawtooth and sinusoidal disturbing signals are considered.

### *Scenario 1: Robustness towards parametric uncertainties*

In this scenario, we propose to evaluate the robustness of the proposed RISE control by considering an uncertainty term $\Delta I_0$ on the parameter $I_0$ and an uncertainty term $\Delta m_0$ on the parameter $m_0$. $I_0$ and $m_0$ represent a combination of several physical parameters as described in (29) and (30). We propose to compare the results with those of the first order sliding mode control proposed in (Khalid and Memon (2016)). The physical parameters of the real benchmark are summarized in **Table** 1. The control gains are summarized in **Table** 2. To analyse the robustness of the RISE control with respect to the sliding mode control, in case of parametric uncertainties, let us consider the following robustness evaluation indices:

- The Integral Square Error (ISE)

$$ISE = \int e_{\theta_1}^2 dt \tag{73}$$

- Integral Absolute Error (IAE)

$$IAE = \int |e_{\theta_1}| dt \tag{74}$$

where $e_{\theta_1}$ denotes the tracking error of the unactuated joint $\theta_1$.

**Table 2.** Summary of the control design parameters.

| Parameters | Value | Parameters | Value |
|---|---|---|---|
| $\alpha_1$ | 15.3 | $I_0$ | 0.0130 |
| $\alpha_2$ | 1.5 | $m_0$ | 0.213 |
| $\beta$ | 14.05 | $K_s$ | 125.0 |
| $\Upsilon_0$ | 1.4800 | $\Theta_0$ | 0.0092 |

In this section the obtained simulation results of the first scenario are presented and discussed. We chose the initial configuration as $[\theta_1, \dot{\theta}_1, \dot{\theta}_2, v_f]^T = [0.2, 0, 0, 0]^T$. The evolution of the system states versus time is depicted in **Figure** 3.

- $\Delta I_0 = 0\%$ and $\Delta m_0 = 0\%$: In this case, no uncertainties are introduced, thus the simulation is performed in nominal case. For the case of RISE controller, we can clearly observe the convergence of the pendulum angle, the pendulum velocity and the inertia wheel velocity to the equilibrium point $[\theta_1, \dot{\theta}_1, \dot{\theta}_2] = [0, 0, 0]$ in a smaller interval of time than the SMC approach. The input torque converges to a zero steady-state value as shown in **Figure** 3(d).
- $\Delta I_0 = 20\%$ and $\Delta m_0 = 20\%$: Despite the introduced uncertainties, no oscillations are produced by the proposed RISE controller compared to the standard SMC. A significant improvement of 79.2% and 83.2% are noticed when evaluating the ISE and IAE robustness indices respectively as reported in **Table** 3.
- $\Delta I_0 = 50\%$ and $\Delta m_0 = 50\%$: By introducing large variations of 50% in the model's parameters $m_0$ and $I_0$, we can clearly notice from simulation results a remarkable difference between the RISE and SMC controllers. The SMC is not able to compensate for the introduced parametric uncertainties. More oscillations around the equilibrium point are observed when increasing the percentage of uncertainties in case of SMC approach. However, it is clear from the results of the proposed RISE that the control approach can compensate for parametric uncertainties. To sum up, we can conclude that the proposed standard RISE controller is more robust towards parametric uncertainties than the SMC one.

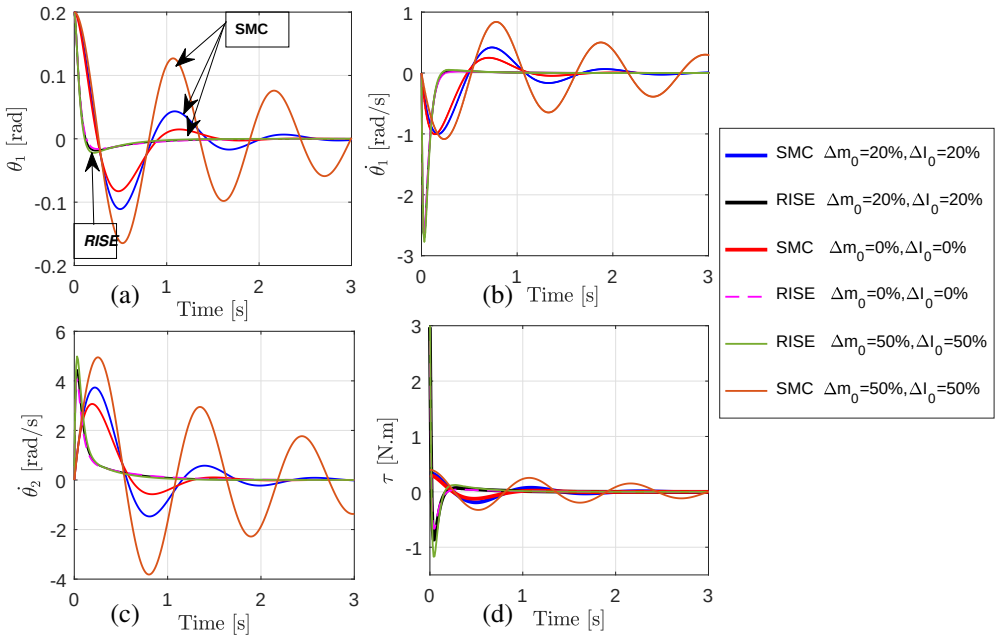


**Figure 3.** Obtained simulation results for scenario 1: Robustness towards parametric uncertainties. (a): pendulum angular position, (b): pendulum angular velocity, (c): velocity of the inertia wheel, (d): control input.

**Table 3.** Control robustness evaluation of the SMC and RISE controllers for scenario 1.

| | IAE | ISE |
|---|---|---|
| SMC $\Delta I_0 = 20\%$,$\Delta m_0 = 20\%$ | 0.0965 | 0.0086 |
| RISE $\Delta I_0 = 20\%$,$\Delta m_0 = 20\%$ | 0.02 | 0.0014 |
| Improvements | 79.2% | 83.2% |

## *Scenario 2: External disturbances rejection*

The first considered perturbation is a non-sinusoidal sawtooth disturbing torque equal to [0.3 Nm] applied to the pendulum at time $t = 4s$ and remaining 3 seconds. The second applied disturbing signal is expressed by $D = 0.1sin(15t) + 0.15$. It has been applied during the interval [10 13] seconds.

The simulation results of the second scenario are displayed in **Figure** 4, where we can see the effect of the disturbances in the evolution of the states. The proposed original RISE controller reacts immediately

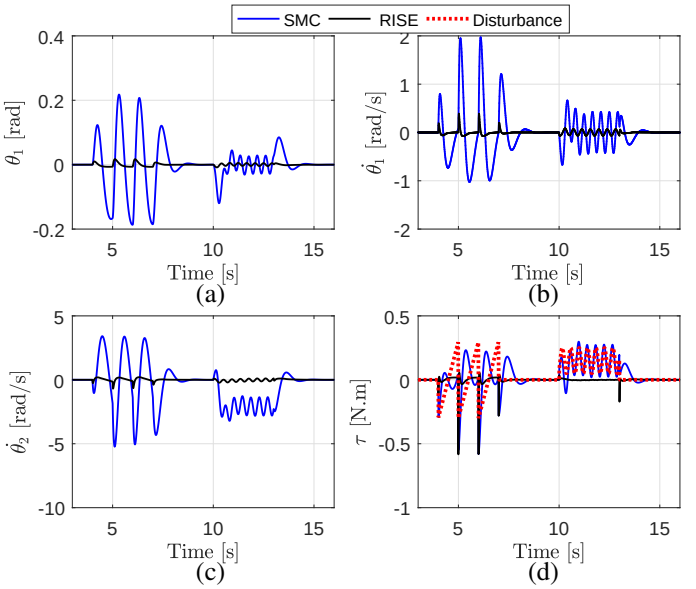


**Figure 4.** Obtained simulation results for scenario 2. (a): Pendulum angular position, (b): pendulum angular velocity, (c): velocity of the inertia wheel, (d)Control input and disturbing signal.

to these disturbances and brings back the states to the desired equilibrium point. The deviation due to the external disturbances is compensated by the control action. The numerical simulation shows the effectiveness of the proposed control approach compared to the SMC especially when the system is subject to the first non-sinusoidal and periodic disturbance. The performance of the proposed control approach is improved by more than 90% as illustrated in **Table** 4. In the next section, we discuss the performance of the proposed controller through real-time experiments.

**Table 4.** Control performance evaluation of the SMC and RISE controllers for scenario 2.

| | IAE | ISE |
|---|---|---|
| SMC | 0.6228 | 0.0728 |
| RISE | 0.0533 | 0.0017 |
| Improvements | 91.4% | 97.7% |

## Real-time experimental results

To validate the performance of the proposed RISE control approach complied with the Levant differentiator, real-time experiments have been performed on the testbed of IWIP designed at LIRMM Laboratory (www.lirmm.fr). The electrical and mechanical components of the experimental testbed are shown in **Figure** 5, for more details about the experimental platform the readers can refer to (Andary et al. (2009); Touati and Chemori (2013); Haddad et al. (2018); Hfaiedh et al. (2020b)).

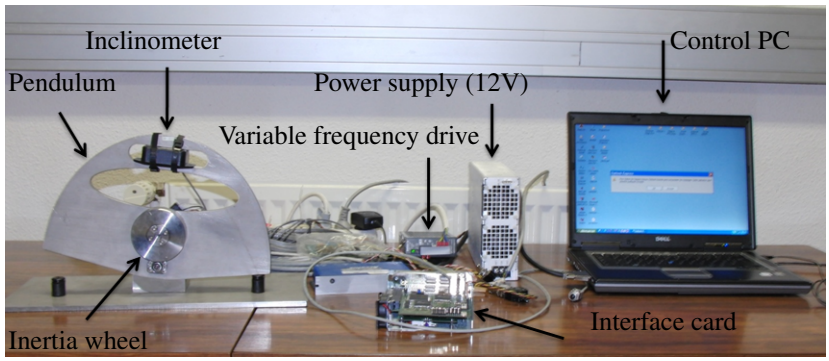


**Figure 5.** View of the IWIP experimental testbed.

**Table 5.** Summary of the control design parameters.

| Parameters | Value | Parameters | Value |
|---|---|---|---|
| $\alpha_1$ | 7.3 | $\hat{\theta}_1(0)$ | 0.16 |
| $\alpha_2$ | 3.2 | $\lambda_0$ | 110 |
| $\beta$ | 14.05 | $\lambda_2$ | 50 |
| $K_s$ | 19.09 | $\lambda_1$ | 80 |

**Remark 2:** The dynamic model of the IWIP in (28) and the one of the experimental model in **Figure** 5 are considered the same. Indeed, there may still a difference between the dynamics of the experimental plant and the mathematical model even with a good identification. For instance, the dynamic model of the actuator and the frictional forces of the system are neglected in the proposed dynamic model of the system. Two experimental scenarios have been performed. In the first one, no external disturbances are considered, that is the experimental validation is achieved in the nominal case.

The proposed observer-based RISE Control, the original RISE and the SMC are compared in nominal case.

In the second scenario, we consider persistent external disturbances. The control design parameters are summarized in **Table** 5. In order to analyse the control performance and to highlight the improvement gained by using the Levant differentiator in terms of tracking error, let us consider the following evaluation indices :

- The root mean square of the tracking error (RMSE)

$$RMSE = (\frac{1}{N}\sum_{i=1}^{N}(e_{\theta_1}(i))^2)^{\frac{1}{2}} \tag{75}$$

where $N$ denotes the number of the recorded samples and $e_{\theta_1}$ denotes the tracking error of the unactuated joint $\theta_1$.

We consider the following input-torque-based criterion in order to analyse the performance of the system in terms of energy consumption

$$E_\tau = \sum_{i=1}^{N}|\tau_{\theta_2}(i)| \tag{76}$$

where $\tau_{\theta_2} = u$ denotes the torque generated by the actuator of the inertia wheel.

### *Scenario 1: Nominal case*

In this section, we present the results of both the SMC, the RISE controller using numerical derivative as well as the obtained results of the proposed extended RISE controller combined with Levant differentiator. The evolution of the angular position $\theta_1$ and velocity of the pendulum $\dot{\theta}_1$ are depicted in **Figure** 6. The results show that all states converge to the unstable equilibrium point. However, the response of the pendulum and the wheel are fast for the case of the original RISE and the proposed approach compared to the first-order SMC approach. For more clarity, the two figures are zoomed within the interval [6.5,7] seconds and [6,7] respectively. The measured states of the standard RISE controller are presented with a solid line and the estimated signals obtained from the differentiator are presented in dash line. We observe a good stabilization of the pendulum around its unstable equilibrium. However, a noticeable difference is highlighted in the zoomed plots between the numerical derivative of the pendulum position and the estimated one generated by the differentiator. We can easily find out that the use of the differentiator attenuates significantly the noise as opposed to the numerical derivative.

The evolution of the control input for the three controllers and the auxiliary error $e_2$ are displayed in **Figure** 7. The plots are zoomed within the interval [10,15] seconds where the solid line represents the results of the proposed control approach and the dashed line represents the results of the standard RISE

without the differentiator. We can also observe an improvement in the signal quality of the estimated auxiliary errors $e_2$ with respect to the measured one.

Although the standard RISE controller ensures a good stabilization of the system, the use of the Levant differentiator leads to an attenuation of noise in the velocity estimation resulting in a smoother control input signal, opposed to the use of numerical derivative which amplifies any embedded noise in the measurement signals. This noise is due, for instance, to some interferences from other electrical sources, hardware, sensors or environment.

To sum up, the real-time experimental results illustrate clearly that the original RISE and the proposed observer-based RISE approach outperform the SMC in terms of convergence. On the other hand, the Levant's differentiator provides a better real-time estimation of the velocity than numerical derivative.

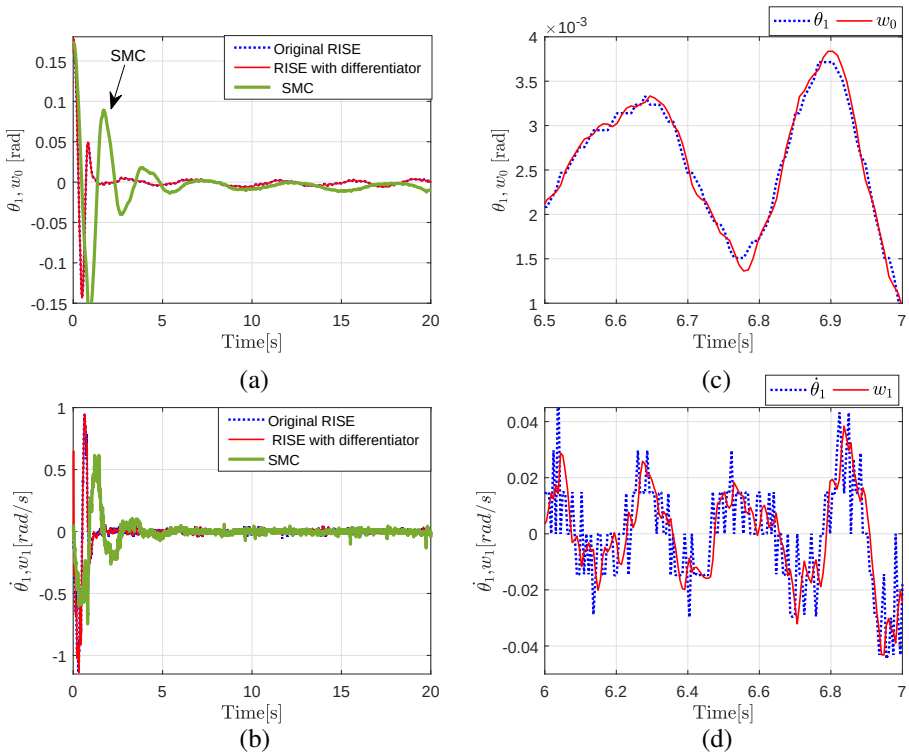


**Figure 6.** Obtained experimental results for the first scenario: nominal case, (a): pendulum angular position, (b): pendulum angular velocity, (c): zoomed-in view of pendulum angular position, (d): zoomed-in view of pendulum angular velocity.

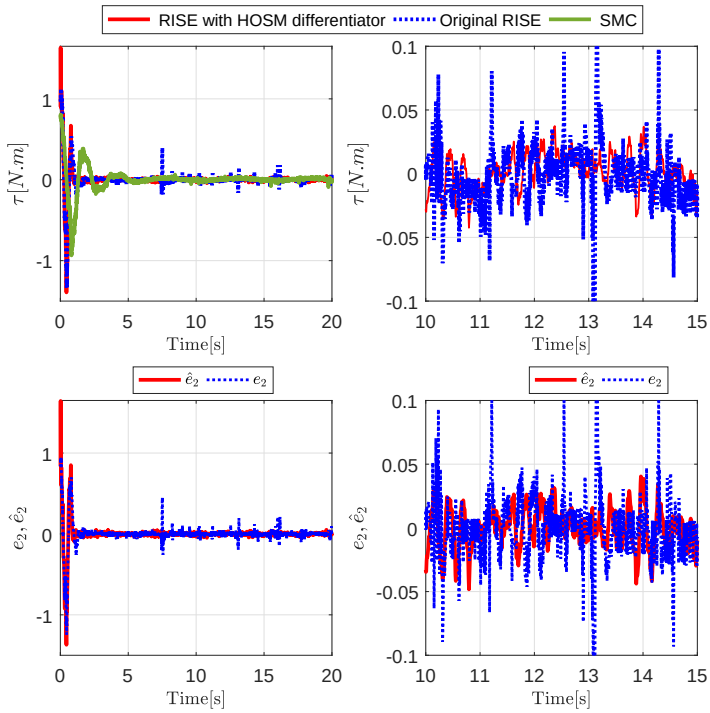


**Figure 7.** Evolution of the control input and the auxiliary error $e_2$ in real-time experiments of scenario 1: Nominal case

**Table 6.** Quantification of the performance through different evaluation criteria for scenario 1.

| Criteria | SMC | Original RISE | Improvements | RISE with differentiator | Improvements |
|---|---|---|---|---|---|
| RMSE [rad] | 0.0051 | 0.0012 | 76.4% | $8.643e^{-4}$ | 82.35 % |
| ISE | 0.0239 | 0.0098 | 59 % | 0.0089 | 62.760 % |
| IAE | 0.3961 | 0.165 | 58.34 % | 0.1548 | 60.92 % |
| $E_\tau[N.m]$ | 189.8981 | 163.96 | 13.66 % | 134.09 | 18.22 % |

To compare the effectiveness of the three approaches, we suggest computing the above performance-evaluation indices. The obtained results are summarized in **Table** 6. The improvements are computed with respect to the SMC approach. Note that, the smallest value of the performance criteria reflects the best performance. This scenario shows clearly that both the proposed observer-based RISE control scheme and the original RISE control one overcome the SMC in terms of convergence and energy consumption. It can be concluded from the obtained results that the RISE controller without differentiator provides

satisfactory results. However, the proposed control scheme has the best performance evaluation indices and improvement compared to the standard RISE approach, thanks to the Levant differentiator.

### *Scenario 2: Persistent disturbances rejection*

The main motivation behind the second scenario is to show the effectiveness of the control approach when the system is under a more complex and more challenging type of disturbances. It consists of two persistent forces generated through an additional mass attached to the pendulum body. The mass was attached during the interval $[10.5, 16.5]$ seconds and $[21, 26]$ seconds. An illustration of added persistent mass can be shown in **Figure** 8. It is an interesting scenario as the added mass create a variation in the dynamic model. Indeed the pendulum mass becomes ($m_* = m + m_{dis}$) where $m_{dis}$ is the added mass. On the other hand, the applied disturbances create an external torque disturbing the pendulum. Compared to the previous work in (Hfaiedh et al. (2018)), the disturbances are not punctual but applied in two consecutive and different periods. It is a more challenging scenario, to evaluate the performance and energy consumption of the proposed control scheme. In this scenario, the original standard RISE controller and the proposed observer based RISE controller are tested and compared. For the purpose of clarity, a zoomed-in view of the evolution of the states within the two intervals is depicted in **Figure** 9. According to these results, we can observe that the persistent disturbances are compensated by both control approaches and the measured position and velocity converge to equilibrium steady states. However, it can be seen from the zoom plots that the differentiator based RISE controller provides better results than the standard RISE controller. We can also point out that the estimation of the angular position of the pendulum and its derivative has an impact on the control input signal and therefore improves the disturbances rejection in the controlled system. These results are verified also by the above proposed quantification of the performance through different evaluation criteria summarized in **Table** 7.

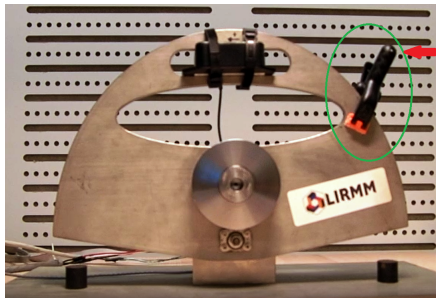


**Figure 8.** Illustration of persistent disturbances.

**Table 7.** Quantification of the performance through different evaluation criteria for scenario 2.

| Criteria | Without Differentiator | With Differentiator | Improvement |
|---|---|---|---|
| RMSE [rad] | $9.265e^{-3}$ | $5.853e^{-3}$ | 36.83% |
| ISE | $14.4905e^{-3}$ | $14.35766e^{-3}$ | 0.92% |
| IAE | $368.0434e^{-3}$ | $322.1330e^{-3}$ | 12.47% |
| $E_\tau[N.m]$ | 218.7362 | 206.8575 | 5.43% |

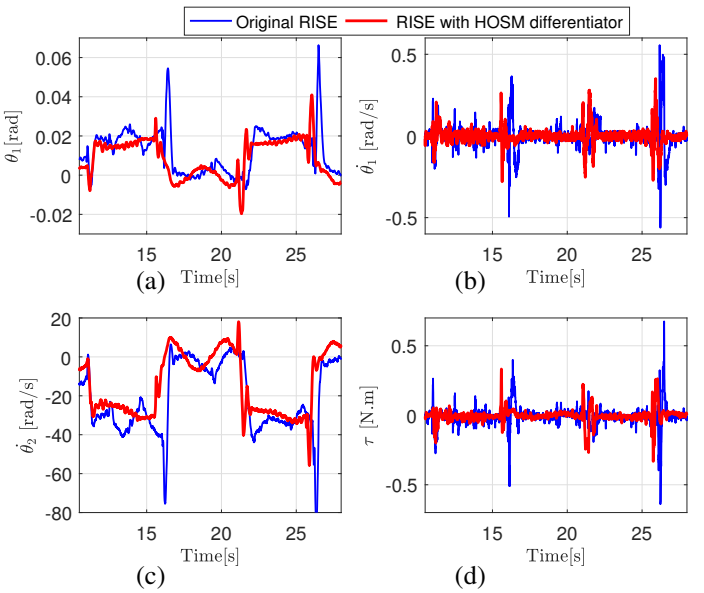


**Figure 9.** Obtained experimental results for scenario2: Rejection of persistent perturbations. (a): Pendulum angular position, (b): pendulum angular velocity, (c): velocity of the inertia wheel, (d) Control input.

## Conclusion and future work

This paper proposes two robust RISE control approaches for the stabilization of class I of underactuated mechanical systems. For the design of the RISE controller, the model of the system is first transformed into a strict-feedback form. With a Lyapunov-based analysis, two new desired trajectories are defined. Then the stability analysis of the resulting closed-loop system and simulation results for different operating conditions were addressed. They attest clearly that the first proposed RISE control approach ensures better stabilization and robustness towards different parametric uncertainties and external disturbances, compared to the SMC approach. However, the limitation of this approach was

experimentally noticed through the amplified noise, resulting from the numerical derivative action in the control law. To overcome this problem, a Levant differentiator was proposed and implemented to estimate the system states, including the time derivative of the angular position. Based on the obtained experimental results and further analysis based on some performance-evaluation indices, the combination of Levant differentiator with RISE controller has significantly attenuated the effect of the noise included in the measured signals and improved the performance in terms of tracking error and energy consumption, compared to original RISE and SMC schemes. In future work, various possible perspectives of this work can be investigated. At first, we can combine an adaptation law with the RISE controller to estimate the gains. Furthermore, the automatic optimal tuning of the control design parameters of the controller can also be considered. Finally, further discussions can be investigated about the generalization of this study to the case of other classes of underactuated mechanical systems.

## Funding

No funds, grants, or other support was received.

## Declaration of conflicting interests

The authors declare that they have no conflict of interest/competing interests.

## References

Aguilar-Avelar C, Rodríguez-Calderón R, Puga-Guzmán S and Moreno-Valenzuela J (2017) Effects of nonlinear friction compensation in the inertia wheel pendulum. *Journal of Mechanical Science and Technology* 31(9): 4425–4433. DOI:10.1007/s12206-017-0843-4.

Andary S, Chemori A, Benoit M and Sallantin J (2012) A dual model-free control of underactuated mechanical systems, application to the inertia wheel inverted pendulum. In: *2012 American Control Conference (ACC)*. Montreal, QC, Canada, pp. 1029–1034. DOI:10.1109/ACC.2012.6315492.

Andary S, Chemori A and Krut S (2009) Control of the underactuated inertia wheel inverted pendulum for stable limit cycle generation. *Advanced Robotics* 23(15): 1999–2014. DOI:10.1163/016918609X12529279062438.

Bennehar M, Chemori A, Bouri M, Jenni L and Pierrot F (2018) A new rise-based adaptive control of pkms: design, stability analysis and experiments. *International Journal of Control* 91(3): 593–607. DOI:10.1080/00207179.2017.1286536.

Cheng CC and Ho CH (2017) Design of adaptive sliding mode controllers for mismatched perturbed systems with application to underactuated systems. In: *2017 36th Chinese Control Conference (CCC)*. Dalian, China, pp. 1329–1336. DOI:10.23919/ChiCC.2017.8027535.

Choukchou-Braham A, Cherki B, Djemai B and M Busawon K (2014) *Analysis and Control of Underactuated Mechanical Systems*. Switzerland: Springer International Publishing.

Ding F, Huang J, Wang Y, Zhang J and He S (2017) Sliding mode control with an extended disturbance observer for a class of underactuated system in cascaded form. *Nonlinear Dynamics* 90: 2571–2582.

Donaire A, Romero JG, Ortega R, Siciliano B and Crespo M (2017) Robust ida-pbc for underactuated mechanical systems subject to matched disturbances. *International Journal of Robust and Nonlinear Control* 27(6): 1000–1016.

Estrada A, Aguilar LT, Iriarte R and Fridman L (2012) Two relay controller for real time trajectory generation and its application to inverted orbital stabilization of inertia wheel pendulum via quasi-continuous hosm. *Asian Journal of Control* 14(1): 58–66. DOI:10.1002/asjc.339.

Fantoni I and Lozano R (2002) *Non-linear Control for Underactuated Mechanical Systems*. New York: Springer, London.

Fischer N, Hughes D, Walters P, Schwartz EM and Dixon WE (2014) Nonlinear rise-based control of an autonomous underwater vehicle. *IEEE Transactions on Robotics* 30(4): 845–852. DOI:10.1109/TRO.2014.2305791.

Freidovich LB, Hera PL, Mettin U, Robertsson A, Shiriaev AS and Johansson R (2009) Shaping stable periodic motions of inertia wheel pendulum: theory and experiment. *Asian Journal of Control* 11(5): 548–556. DOI:10.1002/asjc.135.

Ghommam J and Chemori A (2017) Adaptive rbfnn finite-time control of normal forms for underactuated mechanical systems. *Nonlinear Dyn* 90(1): 301–315.

Gritli H, Khraief N, Chemori A and Belghith S (2017) Self-generated limit cycle tracking of the underactuated inertia wheel inverted pendulum under IDA-PBC. *Nonlinear Dynamics* 89(3): 2195–2226. DOI:10.1007/s11071-017-3578-y.

Guemghar K (2005) *On the use of input-output feedback linearization techniques for the control of nonminimum-phase systems*. PhD Thesis, ecole polytechnique federale de Lausanne, Lausanne, Suisse.

Haddad NK, Chemori A and Belghith S (2018) Robustness enhancement of ida-pbc controller in stabilising the inertia wheel inverted pendulum: theory and real-time experiments. *International Journal of Control* 91(12): 2657–2672. DOI:10.1080/00207179.2017.1331378.

Hfaiedh A, Chemori A and Abdelkrim A (2018) Rise controller for class i of underactuated mechanical systems: Design and real-time experiments. In: *The 3rd International Conference on Electromechanical Engineering (ICEE'2018)*. Skikda, Algeria.

Hfaiedh A, Chemori A and Abdelkrim A (2020a) Disturbance observer-based super-twisting control for the inertia wheel inverted pendulum. In: *17th International Multi-Conference on Systems, Signals and Devices (SSD'20)*. Sfax, Tunisia, pp. 751–756.

Hfaiedh A, Chemori A and Abdelkrim A (2020b) Stabilization of the inertia wheel inverted pendulum by advanced ida-pbc based controllers: Comparative study and real-time experiments. In: *17th International Multi-Conference on Systems, Signals and Devices (SSD'20)*. Sfax, Tunisia, pp. 757–764.

Imine H, Fridman L and Djemai HSM (2011) *Observation and Identification via HOSM-Observers*, volume 414. Berlin, Heidelberg: Springer Berlin Heidelberg. ISBN 978-3-642-22224-5, pp. 5–24.

Jian L, Wen T and Fuchun S (2014) Adaptive rise control of a multi-link flexible manipulator based on integral manifold approach. In: *2014 International Conference on Multisensor Fusion and Information Integration for Intelligent Systems (MFI)*. Beijing, China, pp. 1–6.

Khalid N and Memon AY (2016) Output feedback control of a class of under actuated nonlinear systems using extended high gain observer. *Arabian Journal for Science and Engineering* 41(9): 3531–3542.

Krafes S, Chalh Z and Saka A (2018) A review on the control of second order underactuated mechanical systems. *IEEE Transactions on Automatic Control* 2018: 1–17. DOI:10.1155/2018/9573514.

Krstic M, Kanellakopoulos I and Kokotovic PV (1995) *Nonlinear and Adaptive Control Design*. John wiley and sons edition. John Wiley and Sons.

Levant A (2003) Higher-order sliding modes, differentiation and output-feedback control. *International Journal of Control* 76(9-10): 924–941.

Lu B, Fang Y and Sun N (2016) Global stabilization of inertia wheel systems with a novel sliding mode-based strategy. In: *2016 14th International Workshop on Variable Structure Systems (VSS)*. Nanjing, China, pp. 200–205. DOI:10.1109/VSS.2016.7506916.

Moreno-Valenzuela J, Aguilar-Avelar C, Puga-Guzman S and Santibanez V (2017) Two adaptive control strategies for trajectory tracking of the inertia wheel pendulum: neural networks vis à vis model regressor. *Intelligent Automation & Soft Computing* 23(1): 63–73. DOI:10.1080/10798587.2015.1121618.

Olfati-Saber R (2001) *Nonlinear Control of Underactuated Mechanical Systems with Application to Robotics and Aerospace Vehicles*. PhD Thesis, Massachusetts Institute of Technology, Cambridge, MA, USA.

Ortega R, Spong MW, Gomez-Estern F and Blankenstein G (2002) Stabilization of a class of underactuated mechanical systems via interconnection and damping assignment. *IEEE Transactions on Automatic Control* 47(8): 1218–1233. DOI:10.1109/TAC.2002.800770.

Seto D and Baillieul J (1994) Control problems in super-articulated mechanical systems. *IEEE Transactions on Automatic Control* 39(12): 2442–2453. DOI:10.1109/9.362851.

Sherwani KIK, Kumar N, Chemori A, Khan M and Mohammed S (2020) Rise-based adaptive control for eicosi exoskeleton to assist knee joint mobility. *Robotics and Autonomous Systems* 124: 103354. DOI:https://doi.org/10.1016/j.robot.2019.103354.

Slotine JJE and Li W (1991) *Applied Nonlinear Control*. Prentice-Hall International Editions. Prentice-Hall. ISBN 9780130400499.

Spong MW (1994) Partial feedback linearization of underactuated mechanical systems. *Proceedings of IEEE/RSJ International Conference on Intelligent Robots and Systems (IROS'94)* 1: 314–321,.

Spong MW (1995) The swing up control problem for the acrobot. *IEEE Control Systems Magazine* 15(1): 49–55. DOI:10.1109/37.341864.

Spong MW and Praly L (1997) *Control of underactuated mechanical systems using switching and saturation*. Springer Berlin Heidelberg, pp. 162–172. DOI:10.1007/BFb0036093.

Sun N, Fang Y and Chen H (2015) A novel sliding mode control method for an inertia wheel pendulum system. In: *2015 International Workshop on Recent Advances in Sliding Modes (RASM)*. Istanbul, Turkey, pp. 1–6. DOI:10.1109/RASM.2015.7154585.

Taktak-Meziou M, Chemori A, Ghommam J and Derbel N (2014) A prediction-based optimal gain selection in rise feedback control for hard disk drive. In: *2014 IEEE Conference on Control Applications (CCA)*. Juan Les Antibes, France, pp. 2114–2119.

Thakar PS, Bandyopadhyay B and Gandhi P (2013) Sliding mode control for an underactuated slosh-container system using non-linear model. *Int. J. of Advanced Mechatronic Systems* 5: 335 – 344. DOI:10.1504/IJAMECHS.2013.059794.

Touati N and Chemori A (2013) Predictive control for the stabilization of a fast mechatronic system : from simulation to real-time experiments. *IFAC Proceedings Volumes* 46(5): 237 – 242. 6th IFAC Symposium on Mechatronic Systems.

Utkin VI (2008) *Sliding Mode Control: Mathematical Tools, Design and Applications*. Berlin, Heidelberg: Springer Berlin Heidelberg. ISBN 978-3-540-77653-6, pp. 289–347. DOI:10.1007/978-3-540-77653-6_5. URL https://doi.org/10.1007/978-3-540-77653-6_5.

Xian B, Dawson DM, De Queiroz MS and Chen J (2004) A continuous asymptotic tracking control strategy for uncertain nonlinear systems. *IEEE Transactions on Automatic Control* 49(7): 1206–1211. DOI:10.1109/TAC.2004.831148.

Zhang A, Yang C, Gong S and Qiu J (2016) Nonlinear stabilizing control of underactuated inertia wheel pendulum based on coordinate transformation and time-reverse strategy. *Nonlinear Dynamics* 84(4): 2467–2476.

Zhang M and Tarn TJ (2001) Hybrid control for the pendubot. In: *Proceedings 2001 ICRA. IEEE International Conference on Robotics and Automation (Cat. No.01CH37164)*, volume 2. pp. 2102–2107 vol.2. DOI:10.1109/ROBOT.2001.932917.

Zhao D and Yi J (2006) Ga-based control to swing up an acrobot with limited torque. *Transactions of the Institute of Measurement and Control* 28(1): 3–13. DOI:10.1191/0142331206tm158oa.